Effect of Sn and Sb element on the magnetism and functional properties of Ni–Mn–Al ferromagnetic shape memory alloys

Sandeep Agarwal [a,*,1], P.K. Mukhopadhyay [a]

LCMP, Department of Condensed Matter Physics and Material Sciences, SN Bose National Centre for Basic Sciences, JD Block, Salt Lake, Kolkata 700098, India

Keywords:
Magnetic measurements
Shape memory
Phase transitions
Magnetocaloric
Magnetoresistance
Magnetism

A B S T R A C T

We have replaced Al partially with Sb and Sn in Ni–Mn–Al systems and investigated its effect on magnetism, entropy change and magnetoresistance in the vicinity of martensitic transformation. Both the samples had identical lattice parameters and Mn contents, which are mostly responsible for magnetism in these systems, yet there were marked changes in magnetic and functional properties of these systems. It was found that the magnetization increased in Sb alloy, while entropy change and magnetoresistance decreased as compared to Sn alloy. These changes are attributed to the change in antiferromagnetic interaction as a result of variation in the Ni d–Mn d hybridization arising due to presence of different sp elements.

1. Introduction

The multifunctional properties such as large magnetocaloric effect (MCE), giant magnetoresistance (MR) and large magnetic field induced strain obtained in Ni_2Mn–X (X=Sn, Sb, In) Heusler alloys showing magnetic shape memory effect has attracted great attention in recent decade [1–3]. Large values of these properties are usually obtained in the vicinity of structural transformation temperature, where they are driven by large difference in the Zeeman energy of austenitic and martensitic phase [4].

The Ni–Mn–Al system has better mechanical properties than Ni_2Mn–X system, but this system tends to stabilize into anti-ferromagnetic (AFM) disordered B2 phase upon quenching form high temperature, whereas Ni–Mn–X system in general stabilizes into ordered $L2_1$ phase in which interaction is predominantly ferromagnetic (FM). The presence of B2 structure in austenitic phase reduces the functional capabilities of these alloys [5,6]. Previous work has shown that it is possible to obtain lager functional capabilities in the Ni–Mn–Al system by replacing Al with X element and giving proper heat treatment [7,8]. The presence of X element stabilizes the $L2_1$ phase in the system and with proper heat treatment $L2_1$ fraction can be further increased [9,10]. Sn and Sb based system display least change in martensitic transformation temperature with variation in X concentration [11]. Thus these two systems were selected for the substitution give us better control over the transformation temperature. We studied how properties such as magnetism, MC and MR get affected and thus tried to determine which system is better suited for the substitution. Such substitution further becomes interesting because of the fact that upon substitution of X with an element of smaller radii, structural transformation temperature of the system increases. This increase occurs even though the e/a ratio system decreases, as the compression of lattice parameter creates internal pressure, thus offering a way to control the transformation temperature [12].

The main contribution to magnetism in Ni–Mn–X FSMA alloys comes from the interaction between the Mn atoms. The interaction is sensitive to the distance that is predominantly FM in austenitic phase ($L2_1$) and is competing AFM/FM in martensitic phase [13]. Recent experimental and theoretical work on Ni_2Mn–In system indicate that the origin of AFM interaction in martensitic phase is superexchange in nature and these interactions mediates through Ni-3d orbitals. In stoichiometric sample (Ni_2MnX) it is ferromagnetic in nature between Mn atoms in the regular Mn site (stoichiometric) and in off-stoichiometric sample with excess Mn it is AFM between Mn atom in regular Mn site and Mn atom in X site [14,15]. Khan et al. have shown that replacement of Cr with Mn in $Ni_{50}Mn_{37-x}Cr_xSb_{13}$ (x=1–6) reduces AFM interaction and argued that it occurs because of weakening of Ni–Mn hybridization [16]. But changing Mn content with increasing Cr content and possibility of Cr occupying Ni, Mn and X site leaves other possibilities affecting magnetism wide open. For example previous study by the same authors on Ni–Mn–Sb system showed that exchange bias effect increased with increase in Mn content,

* Corresponding author.
E-mail address: sandeepxag@yahoo.co.in (S. Agarwal).
[1] Presently at: Haldia Institute of Technology, Haldia, Purba Medhinipur-721657, West Bengal, India.

showing that change in AFM interaction in Cr replaced system can possibly also be outcome of decrease in Mn content [17]. To avoid confusion, here we have studied systems with composition $Ni_2Mn_{1.36}Sb_{0.40}Al_{0.24}$ and $Ni_2Mn_{1.36}Sn_{0.40}Al_{0.24}$, where Mn and Ni content both remain same and systems have almost identical lattice parameter. Hence such study will make comparison of Ni–Mn hybridization more pertinent and may lead to better understanding of magnetism in Ni–Mn–X system.

Usually the comparison of magnetic properties of the systems with different fractions of X elements is hindered by the fact that the electron concentration and Mn–Mn distance (lattice parameter) both changes with the change in composition. Since only *e*/*a* ratio changes in here, our study will help to understand the underlying mechanism of the functional capabilities in these systems and thus pave the way for development of better FSMA.

2. Method and results

Samples of compositions $Ni_2Mn_{1.36}Sn_{0.40}Al_{0.24}$ and $Ni_2Mn_{1.36}Sb_{0.40}Al_{0.24}$ were prepared. The details of sample preparation and magnetic measurement technique are given in Refs. [8,12]. The resistivity measurements were performed using four probe technique in 10 T and 14 T setups from Cryogenics™.

The XRD pattern obtained at room temperature for $Ni_2Mn_{1.36}Sb_{0.40}Al_{0.24}$ is shown in Fig. 1. Rietveld refinement of the sample showed that it was in austenitic phase with $L2_1$ structure and lattice parameter of 0.593 nm. The XRD pattern of $Ni_2Mn_{1.36}Sn_{0.40}Al_{0.24}$ was given in Ref. [12]. It had $L2_1$ structure and the lattice parameter was 0.593 nm. The structural transformation temperatures were determined form DSC curves as shown in Fig. 2. The martensite start (M_s), martensite finish (M_f), austenite start (A_s) and austenite finish (A_f) temperatures for the Sb and Sn systems were found to be 189 K, 154 K, 158 K and 207 K, and 171 K, 158 K, 168 K, and 196 K respectively [12]. The M_s of the Sb alloy was slightly higher than that of Sn. This is consistent with the fact that with increase in electron concentration the transformation temperature increases. As per phenomenological theory of martensitic transformation, thermal hysteresis with slope indicates presence of boundary friction, elastic strain energy and interfacial energy. Narrow thermal hysteresis indicated that there is lesser boundary friction, whereas the larger elastic strain energy and interfacial energy resist the martensitic and reverse transformation leading to larger slope of transformation [18,19]. It was found

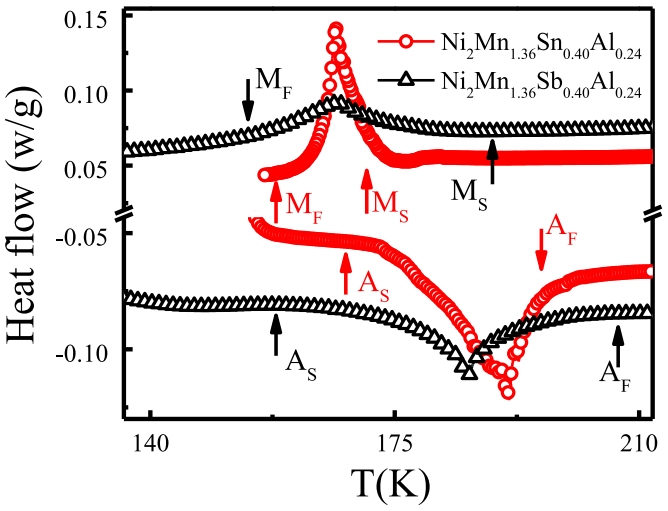

Fig. 2. DSC curves obtained for Sn and Sb based samples in cooling and heating cycle performed at the rate of 10 K/min.

that under same heating and cooling rates, the thermal hysteresis in case of $Ni_2Mn_{1.36}Sn_{0.40}Al_{0.24}$ alloy was 10 K ($\Delta T_H = A_s - M_f$) where as it was 4 K for $Ni_2Mn_{1.36}Sb_{0.40}Al_{0.24}$. Narrow thermal hysteresis in case of Sb alloy indicates that there is lesser boundary friction as compared to Sn alloy. The slope of transformation was found to be greater in case of Sb alloy. This indicates that Sb system will have better phase transition response time and more strain energy across MT.

The Curie temperature (T_C) of Sb alloy was found to be 355 K, while that of Sn alloy was 326 K [12]. Higher T_C in case of Sb alloy shows that the presence of Sb enhances ferromagnetic exchange. Magnetization measurements were performed at 300 K till the field of 1.5 T for both the samples and the obtained *M*–*H* curve is shown in Fig. 3. It can be seen that the magnetic moment of Sn system is 1.60 μ_B/f.u. and that of Sb based system is 1.73 μ_B/f.u., which is higher in case of Sb system. In Ni_2Mn–X system magnetism is mostly carried by Mn atom. Both the systems are in ordered $L2_1$ structure with similar lattice parameters and same contents of Ni and Mn, the only difference is that they have different atoms on the X sites. The presence of different atoms at X site effects hybridization between the Mn–Ni–Mn atoms differently, which in turn effects the interaction among the different Mn

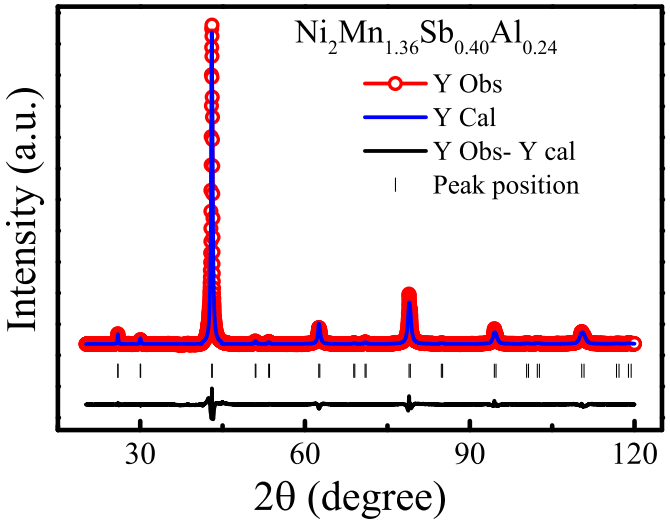

Fig.1. XRD pattern obtained at 300 K alone with calculated pattern, residue and peak position.

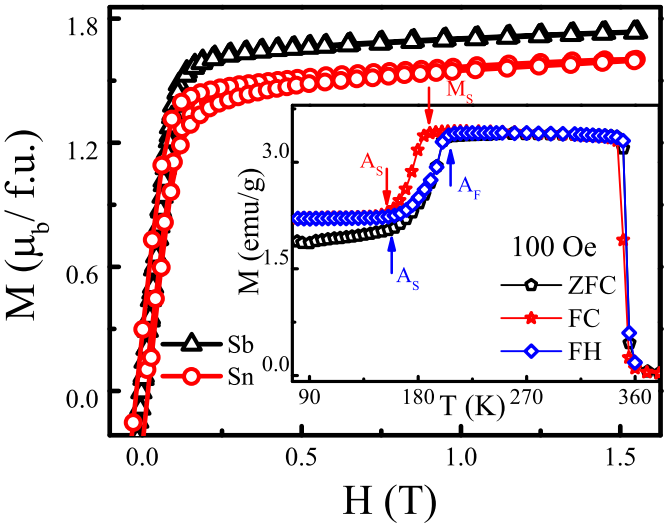

Fig. 3. Magnetic isotherms measured at 300 K for Sn and Sb samples in μ_B/f.u. Inset shows ZFC, FC, and FH at the field of 100 Oe as the function of temperature.

atoms. This possibly gives rise to difference in magnetization of two systems.

The results of Zero-field-cooled (ZFC), field-cooled (FC), and field-heated (FH) thermo-magnetization (MT) measurements for Sb sample performed at the field of 100 Oe are given in inset of the Fig. 3. Similar curves for Sn sample measured at the field of 500 Oe were given in Ref. [11]. The transformation temperatures obtained from DSC are marked in the figure. It can be seen that magnetization measurement shows hysteresis and samples have lower magnetization in the martensitic phase. The structural transformation changes the lattice parameter, thus the Mn–Mn distance in the martensitic phase changes which results in enhancement of AFM interaction and drop in magnetization of martensitic phase [13]. The samples transforms from the dominant FM state (austenitic) to a state with lower magnetization (martensitic) within a few Kelvin. This results in large change in magnetization (ΔM) across martensitic transformation giving rise to properties like inverse magnetocaloric effect and giant magnetoresistance. The magnetocaloric effect was calculated from isothermal magnetization measurements using modified Maxwell's relation $\Delta S_M = \int_{T_1}^{T_2} [\frac{\partial M}{\partial T}]_H dH$ for the system $Ni_2Mn_{1.36}Sn_{0.40}Al_{0.24}$ in Ref. [8]. The isothermal magnetization (M–H) measurements were performed till the field of 1.5 T for $Ni_2Mn_{1.36}Sb_{0.40}Al_{0.24}$ around the martensitic transformation in the warming cycle at a temperature interval of 3 K. To make sure that sample was completely in martensitic phase it was cooled to temperature below the M_f. The obtained values of entropy change (ΔS) are plotted in Fig. 4 along with the ones obtained for Sn based alloy. The maximum of ΔS obtained in case of Sn alloy was 5.6 J kg^{-1} K^{-1} and was 0.365 J kg^{-1} K^{-1} in Sb alloy. The refrigerant capacity (RC) which is defined as the amount of heat transferred in a single thermodynamic cycle from the cold end at T_1 to the hot end at T_2, was calculated by integrating the ΔS_M–T curve over the full width at half maximum using the relation $RC = \int_{T_1}^{T_2} \Delta S_M(T)_H dT$. Obtained values of RC for the field of 1.5 T are 25.2 and 6.8 J kg^{-1} respectively for Sn and Sb alloys.

The ΔM obtained from the M–H curve in Sn alloy was 19.5 emu/g and in case of Sb alloy is only 4 emu/g, it can be seen that even though magnetization is higher in case of Sb the value of ΔM is much lesser. Recent experimental and theoretical work has shown that increased Ni–Mn hybridization leads to stronger AFM interaction, between the Mn atom, occupying Mn site and X site, in martensitic phase [14,15]. The replacement of Sn with Sb most probably weakens the hybridization between the Mn–Ni–Mn thus resulting in enhancement of ferromagnetism in the Sb alloy compared to Sn alloy. The effect is more pronounced in the martensitic phase and as a result of it the value of ΔM is lower in case of Sb alloy. The lower value of ΔM thus results in lower value of ΔS and RC in the Sb sample.

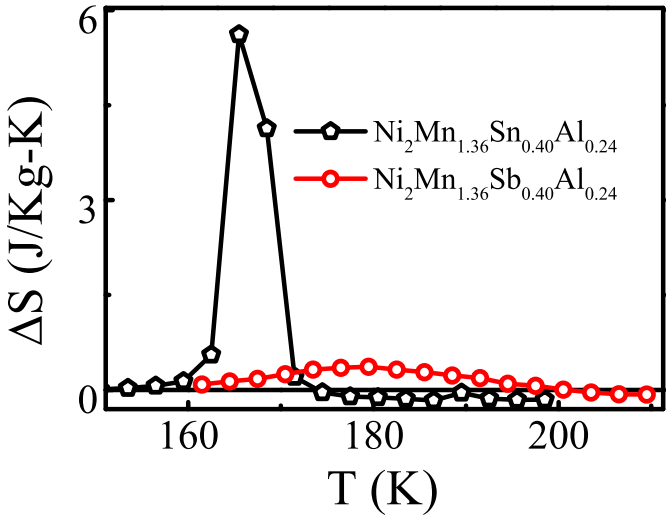

Fig. 4. Entropy change due to application of field of 1.5 T calculated form modified Maxwell relation.

The resistivity measurements were performed in cooling and heating cycles for Sn and Sb alloys as a function of temperature. Fig. 5(a) shows the curves obtained for 0 T and 10 T for Sn sample and Fig. 5(b) shows the curves obtained for 0 T and 14 T for Sb alloy. The resistivity showed sharp changes upon structural transformation. The resistivity of the martensitic phase (ρ_M) is higher than austenitic phase (ρ_A) by ($\Delta\rho_{M-A}=(\rho_M-\rho_A)/\rho_A$) 37% and 32% for Sn and Sb alloys respectively. The structural transformation to martensitic phase enhances the AFM interaction by change in the density of state at Fermi surface. The different magnetic ordering (AFM) and crystal structure in the martensitic phase compared to that of austenitic phase establishes different kind of electronic band structure. This gives rise to super zone gap upon martensitic transformation thus leading to increase in resistance [16,20,21]. The value of $\Delta\rho_{M-A}$ is not much different for Sn and Sb alloy (compared to ΔM and ΔS), which shows that change in magnetic interaction is not solely responsible for increase in resistivity upon MT. It is rather outcome of the combined contributions due to change in magnetic scattering and scattering from the various orientations of martensitic variants [19,22]. The lower value of $\Delta\rho_{M-A}$ in Sb alloy shows that AFM interaction is weak in this system. The resistivity curve measured under dc field, shifts to lower temperature. The shift is large in Sn alloy compared to Sb alloy. The lowering to transformation temperature with field can be understood from Clausius–Clapeyron relation [3]. As the magnetization change in Sb alloy is much smaller than Sn alloy, the resulting shift in transformation temperature is also lower. The drop in MT with field also results in large magnetoresistance ($MR=[\rho(H, T)-\rho(0, T]/\rho(0, T)$. The MR obtained for both samples are given in the Fig. 5(c) and (d). For Sn alloy the maximum MR of 36% is observed for the applied field of 10 T whereas the maximum for Sb alloy is much lower and comes out to 5% for the field of 14 T, even though both the alloy have slightly different change of $\Delta\rho_{M-A}$ upon MT. The MR results are consistent with the magnetic measurements.

So we find that upon substituting Sn with Sb, the magnetization of austenitic phase increases but the change in magnetization across MT decreases. The effect of substitution is even more pronounced on the functional properties like MCE and MR where they decrease by an order of magnitude. The increase in magnetization of Sb alloy shows that the AFM interaction in the sample weakens in austenitic phase. The lowering of ΔM, MCE and MR further shows that the decrease in AFM interaction is more pronounced in martensitic phase than in austenitic phase. The AFM interaction in martensitic phase has been attributed to Ni 3d–Mn 3d hybridization which is sensitive to distance. The XRD results show that the lattice parameter does not change upon substitution of Sn with Sb. The replacement of Sn with Sb leads to increase in the electrons in conduction band. It was argued by Khan et al. that change in electron concentration influences metallic radii of Mn [16,23]. The radii of Mn decreases with increase in electron concentration which will reduce in Ni–Mn distance compared to Sn in Sb, thus the Mn–Ni–Mn hybridization decreases, reducing the AFM interaction in the Sb sample.

3. Discussion

In summary, we have shown that it is possible to obtain large fraction of $L2_1$ phase by replacing Al with other *sp* elements having

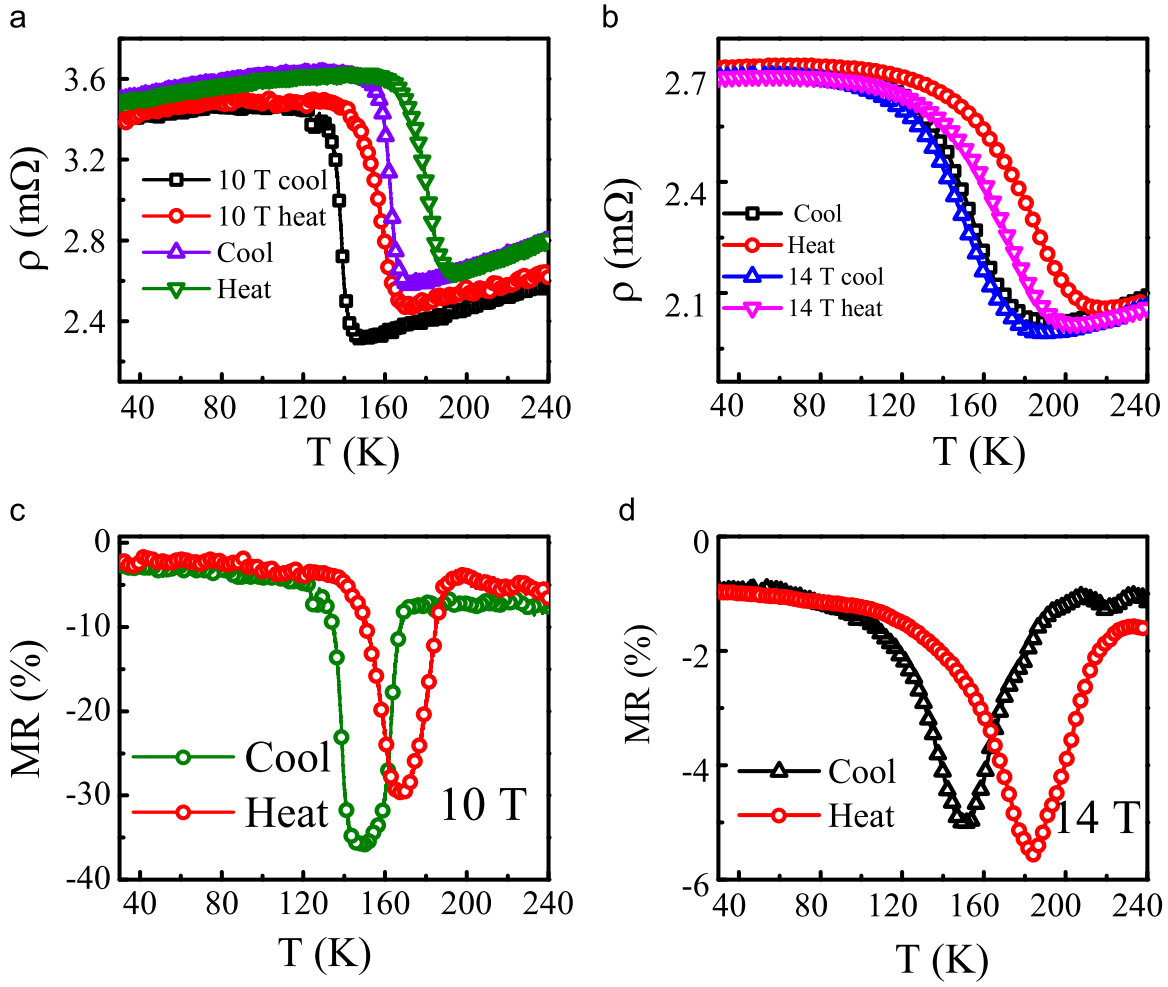

Fig. 5. (a) and (b) show resistivity measurement performed in the zero applied dc magnetic field and field of 10 T and 14 T for Sn and Sb alloy respectively. (c) and (d) show MR obtained for respective alloys.

larger radii. Such replacement also offers us way to control the magnetic and functional properties of these systems. We have also shown the effect that *sp* element can have on the magnetism and properties like MCE and MR. The presence of Sb weakens the AFM interaction in system leading to increase in magnetism of both austenitic and martensitic phases, the effect being more pronounced in martensitic phase. This leads to decrease in magnitude of ΔM, MCE and MR by more than an order. It was further found from the electrical transport measurements that change in magnetic interaction is not solely responsible for the resistivity change in the present systems and there is large contribution from scattering form the different orientation of martensitic variants. Overall it is found that Sn based system are more suitable for MCE and MR devices whereas Sb based alloys is expected to be more suitable for mechanical devices.

Acknowledgments

One of the authors, S.A. would like to thank CSIR, India for financial support as SRF. Authors are thankful to UGC-DAE Kolkata and AK Raychaudhuri for helping with magneto resistance measurement.

References

[1] T. Krenke, E. Duman, M. Acet, E.F. Wassermann, X. Moya, L. Mañosa, et al., Inverse magnetocaloric effect in ferromagnetic Ni–Mn–Sn alloys, Nat. Mater. 4 (2005) 450–454, http://dx.doi.org/10.1038/nmat1395.

[2] K. Koyama, H. Okada, K. Watanabe, T. Kanomata, R. Kainuma, W. Ito, et al., Observation of large magnetoresistance of magnetic Heusler alloy Ni[sub 50]Mn[sub 36]Sn[sub 14] in high magnetic fields, Appl. Phys. Lett. 89 (2006) 182510, http://dx.doi.org/10.1063/1.2374868.

[3] R. Kainuma, Y. Imano, W. Ito, Y. Sutou, H. Morito, S. Okamoto, et al., Magnetic-field-induced shape recovery by reverse phase transformation, Nature 439 (2006) 957–960, http://dx.doi.org/10.1038/nature04493.

[4] H.E. Karaca, I. Karaman, B. Basaran, Y. Ren, Y.I. Chumlyakov, H.J. Maier, Magnetic field-induced phase transformation in NiMnCoIn magnetic shape-memory alloys – a new actuation mechanism with large work output, Adv. Funct. Mater. 19 (2009) 983–998, http://dx.doi.org/10.1002/adfm.200801322.

[5] X. Moya, L. Mañosa, A. Planes, T. Krenke, M. Acet, M. Morin, et al., Temperature and magnetic-field dependence of the elastic constants of Ni–Mn–Al magnetic Heusler alloys, Phys. Rev. B 74 (2006) 024109, http://dx.doi.org/10.1103/PhysRevB.74.024109.

[6] M. Acet, E. Duman, E.F. Wassermann, L. Mañosa, A. Planes, Coexisting ferro- and antiferromagnetism in Ni[sub 2]MnAl Heusler alloys, J. Appl. Phys. 92 (2002) 3867, http://dx.doi.org/10.1063/1.1504498.

[7] S. Agarwal, E. Stern-Taulats, L. Mañosa, P.K. Mukhopadhyay, Effect of low temperature annealing on magneto-caloric effect of Ni–Mn–Sn–Al ferromagnetic shape memory alloy, J. Alloy. Compd. 641 (2015) 244–248, http://dx.doi.org/10.1016/j.jallcom.2015.04.069.

[8] S. Agarwal, P.K. Mukhopadhyay, The effect of Al replacement and heat treatment on magnetocaloric properties of Ni_2Mn–Sn ferromagnetic shape memory alloys, J. Alloy. Compd. 608 (2014) 329–333, http://dx.doi.org/10.1016/j.jallcom.2014.04.095.

[9] E. Wachtel, F. Henninger, B. Predel, Constitution and magnetic properties of Ni–Mn–Sn alloys – solid and liquid state, J. Magn. Magn. Mater. 38 (1983) 305–315, http://dx.doi.org/10.1016/0304-8853(83)90372-4.

[10] T. Miyamoto, W. Ito, R.Y. Umetsu, R. Kainuma, T. Kanomata, K. Ishida, Phase stability and magnetic properties of $Ni_{50}Mn_{50-x}In_x$ Heusler-type alloys, Scr. Mater. 62 (2010) 151–154, http://dx.doi.org/10.1016/j.scriptamat.2009.10.006.

[11] Y. Sutou, Y. Imano, N. Koeda, T. Omori, R. Kainuma, K. Ishida, et al., Magnetic and martensitic transformations of NiMnX(X=In,Sn,Sb) ferromagnetic shape

memory alloys, Appl. Phys. Lett. 85 (2004) 4358, http://dx.doi.org/10.1063/1.1808879.
[12] S. Agarwal, S. Banerjee, P.K. Mukhopadhyay, Crossover of spin glass characteristics as a function of field in an NiMnSnAl alloy, J. Appl. Phys. 114 (2013) 133904, http://dx.doi.org/10.1063/1.4823782.
[13] P.J. Brown, A.P. Gandy, K. Ishida, R. Kainuma, T. Kanomata, K.U. Neumann, et al., The magnetic and structural properties of the magnetic shape memory compound $Ni_2Mn_{1.44}Sn_{0.56}$, J. Phys. Condens. Matter 18 (2006) 2249–2259, http://dx.doi.org/10.1088/0953-8984/18/7/012.
[14] K.R. Priolkar, P.A. Bhobe, D.N. Lobo, S.W. D'Souza, S.R. Barman, A. Chakrabarti, et al., Antiferromagnetic exchange interactions in the Ni_{2}Mn_{1.4}In_{0.6} ferromagnetic Heusler alloy, Phys. Rev. B 87 (2013) 144412, http://dx.doi.org/10.1103/PhysRevB.87.144412.
[15] K.R. Priolkar, D.N. Lobo, P.A. Bhobe, S. Emura, A.K. Nigam, Role of Ni–Mn hybridization in the magnetism of the martensitic state of Ni–Mn–In shape memory alloys, EPL Eur. Lett. 94 (2011) 38006, http://dx.doi.org/10.1209/0295-5075/94/38006.
[16] M. Khan, I. Dubenko, S. Stadler, J. Jung, S.S. Stoyko, A. Mar, et al., Enhancement of ferromagnetism by Cr doping in Ni–Mn–Cr–Sb Heusler alloys, Appl. Phys. Lett. 102 (2013) 112402, http://dx.doi.org/10.1063/1.4795627.
[17] M. Khan, I. Dubenko, S. Stadler, N. Ali, Exchange bias behavior in Ni–Mn–Sb Heusler alloys, Appl. Phys. Lett. 91 (2007) 072510, http://dx.doi.org/10.1063/1.2772233.
[18] W.-H. Wang, J.-L. Chen, Z. Liu, G.-H. Wu, W.-S. Zhan, Thermal hysteresis and friction of phase boundary motion in ferromagnetic $Ni_{52}Mn_{23}Ga_{25}$ single crystals, Phys. Rev. B 65 (2001) 012416, http://dx.doi.org/10.1103/PhysRevB.65.012416.
[19] J. Dubowik, K. Załęski, I. Gościańska, H. Głowiński, A. Ehresmann, Magnetoresistance and its relation to magnetization in $Ni_{50}Mn_{35}Sn_{15}$ shape-memory epitaxial films, Appl. Phys. Lett. 100 (2012) 162403, http://dx.doi.org/10.1063/1.4704562.
[20] B. Zhang, X.X. Zhang, S.Y. Yu, J.L. Chen, Z.X. Cao, G.H. Wu, Giant magnetothermal conductivity in the Ni–Mn–In ferromagnetic shape memory alloys, Appl. Phys. Lett. 91 (2007) 012510, http://dx.doi.org/10.1063/1.2753710.
[21] V. Antonov, A. Perlov, P. Oppeneer, A. Yaresko, S. Halilov, Mechanism of the giant magnetoresistance in UNiGa from first-principles calculations, Phys. Rev. Lett. 77 (1996) 5253–5256, http://dx.doi.org/10.1103/PhysRevLett.77.5253.
[22] V.K. Srivastava, R. Chatterjee, R.C. O'Handley, Effect of twin boundaries on electrical transport in a Ni–Mn–Ga single crystal, Appl. Phys. Lett. 89 (2006) 222107, http://dx.doi.org/10.1063/1.2397541.
[23] W.B. Pearson, The Crystal Chemistry and Physics of Metals and Alloys, Wiley-Interscience, United States, 1972 ⟨http://books.google.co.in/books/about/The_crystal_chemistry_and_physics_of_met.html?id=jE1RAAAAMAAJ&pgis=1⟩ (accessed 14.07.14).